

Research Article

Open Access



<sup>1</sup> Uzhgorod National University, st. Voloshina,  
54, Uzhhorod, 88000, Ukraine.

Contacts of Authors



\* To whom correspondence should be  
addressed: Alexander Shuaibov

**Citation:** Shuaibov A, Minya A, Malinina A,  
Malinin A, Gomoki Z (2020). Synthesis of  
aluminum oxide nanoparticles in overstressed  
nanosecond discharge plasma with the ectonic  
sputtering mechanism of aluminum electrodes.  
Highlights in BioScience Volume 3. Article ID  
20211. doi:10.36462/H.BioSci.20211

**Received:** May 20, 2020

**Accepted:** July 18, 2020

**Published:** July 27, 2020

**Copyright:** © 2020 Shuaibov et al. This is an  
open access article distributed under the terms  
of the [Creative Commons Attribution License](#),  
which permits unrestricted use, distribution,  
and reproduction in any medium, provided the  
original author and source are credited.

**Data Availability Statement:** All relevant data  
are within the paper and supplementary  
materials

**Funding:** The authors have no support or  
funding to report.

**Competing interests:** The authors declare that  
they have no competing interests.

## Synthesis of aluminum oxide nanoparticles in overstressed nanosecond discharge plasma with the ectonic sputtering mechanism of aluminum electrodes

Alexander Shuaibov<sup>1\*</sup>, Alexander Minya<sup>1</sup>, Antonina Malinina<sup>1</sup>, Alexander Malinin<sup>1</sup> and Zoltan Gomoki<sup>1</sup>

### Abstract

The results of studying the conditions of synthesis and luminescence of aluminum oxide nanoparticles in a plasma of an overstressed nanosecond discharge ignited between aluminum electrodes at an interelectrode distance of 2 mm and air pressure in the range of 50–202 kPa are presented. It was shown that the plasma of the investigated discharge is characterized by a wide luminescence band in the spectral range of 300–430 nm, which is associated with the formation of F and F<sup>+</sup> centers. The research results can be used in micro-nanotechnology, biomedical engineering to obtain nanostructured alumina substrates, on which other nanodevices and films from biomaterials can be placed. The aim of the work was to establish the possibility of detecting small nanoparticles - aluminum oxide nuclei by emission spectroscopy methods and the synthesis of nanostructured alumina films under atmospheric conditions (without the use of vacuum technology) over a large area.

**Keywords:** Luminescence, Nanostructures, Aluminum oxide, Nanosecond overstressed discharge, Argon, Air.

### Introduction

The results of a study of the characteristics and kinetics of processes in a heterogeneous plasma based on mixed flows of a buffer gas -argon, an oxidizing agent (water molecules), and aluminum dust are presented by Bityurin et al. [1, 2]. We studied the plasma of glow and pulsed discharges, as well as a combined high-frequency discharge in mixtures of argon, water vapor, and aluminum dust. In such plasma, the gas component, liquid droplets, solids, and plasma simultaneously coexist. These studies are related to the search for effective and cheap hydrogen production technologies based on the plasma-chemical oxidation of aluminum in water vapor. As a result of such a stimulated process, aluminum dioxide is formed on the high-voltage electrode in the form of a developed scaly surface and thermal energy is released [1, 3]. Moreover, the price of obtaining a hydrogen molecule does not exceed 1.5 eV/molecule, which is much more economical than the hydrolysis method of producing hydrogen. It is of interest, in order to simplify the design of the reactor, to replace the generator of aluminum dust with a size of tens of microns by producing microdroplets of aluminum by exploding micropoints on the surface of aluminum electrodes in a strong electric field of a nanosecond discharge (ecton formation [4]). The electric and optical characteristics of a spark discharge, the current and voltage of which had an oscillatory shape in the microsecond range, are given in Walters et al. [5]. A discharge was ignited between aluminum and graphite electrodes in air and was

investigated by time-resolved emission spectroscopy. The studies were conducted in the ignition mode of the discharge far from the overstress of the discharge gap. Pairs of electrode materials entered the plasma as a result of sputtering under the influence of a spark discharge (the duration of a train of current oscillations was approximately 25  $\mu$ s, and one full oscillation was 5-6  $\mu$ s).

Alumina nanopowders were synthesized by the gas-phase method, in which a drop of molten aluminum was held by a high-frequency field [6]. The drop was streamlined by a stream of argon and oxygen, aluminum vapors were carried away into the colder zone, where they condense and oxidize. The resulting alumina powder was collected on a filter. To obtain nanostructured ceramics, powders with particle sizes of 60 and 15 nm were pressed and annealed in air. The luminescence of F, F<sup>+</sup> centers created by oxygen vacancies in Al<sub>2</sub>O<sub>3</sub> and Al<sub>2</sub>O<sub>3</sub>-C crystals was studied upon excitation by synchrotron radiation with an energy in the range of 3.7 - 15 eV. At a temperature of 300 K, intense luminescence bands were recorded with maxima at wavelengths of 414 nm (F centers) and 330 nm (F<sup>+</sup> centers) when crystals were excited by synchrotron radiation with an energy in the range 4.82–8.66 eV. The decay time of the luminescence of the F<sup>+</sup> centers is 2.0–2.3 ns [7].

Sapphire and nanostructured ceramics have high thermal, mechanical, and chemical stability (the melting point of sapphire is 20500 C) [8]. They are also characterized by increased radiation resistance, which is important when using the appropriate substrate microcircuits intended for use in space and nuclear power plants. The luminescence of radiation-induced sapphire defects under the influence of a pulsed beam based on H<sup>+</sup> / C<sup>+</sup> ions with an energy of 300 keV was studied. It was found that, along with the F and F<sup>+</sup> centers, more complex aggregate centers of the F<sub>2</sub> type are also observed [9]. Using a subnanosecond high-voltage discharge between aluminum electrodes in air, the atmospheric pressure aluminum plasma characteristics were studied with the ecton mechanism for the injection of aluminum vapor into the discharge gap [10]. The production of electrode material vapors in the form of colored plasma jets based on iron and aluminum vapors was most effective in the absence of mismatch of nanosecond voltage pulses and discharge gap resistance. Under these conditions, the deposition of structures based on atomized copper electrodes 1-10 in length and 1  $\mu$ m in diameter was observed on the walls of the discharge chamber.

Currently, there is practically no work on the synthesis of alumina-based nanostructures using an overstressed nanosecond atmospheric pressure discharge with an ecton mechanism [4] for the injection of aluminum vapor into an oxygen-containing gas plasma. The results of such studies of the synthesis conditions and some characteristics of the nanostructures of copper, zinc, and iron oxides are given in [11-14].

This study presents the results of characteristics and parameters of an overstressed nanosecond atmospheric pressure discharge in air and argon at atmospheric pressure between aluminum electrodes and the luminescence characteristics of aluminum oxide nanostructures that were synthesized under the conditions of this experiment.

## Materials and Methods

### Technique and experimental conditions.

An overstressed nanosecond discharge in air and argon was ignited in a sealed 3-liter dielectric chamber between aluminum electrodes. A diagram of the discharge module and device for the synthesis of thin films of transition metal oxides is given in previous research [13-14]. The diameter of the cylindrical aluminum electrodes was 5 mm. The radius of the rounded working end of the aluminum electrodes was 3 mm. Air and argon pressure varied in the range of 50 - 202 kPa. The distance between the electrodes was 2 mm. Aluminum vapor was introduced into the discharge gap due to microexplosions of the inhomogeneities of the surface of aluminum electrodes in a strong electric field of the discharge and the formation of ectons [4]. To ignite the discharge, high voltage bipolar pulses with a total duration of 50-100 ns and an amplitude of  $\pm$  (20-40) kV were applied to the electrodes. The discharge was photographed using a digital camera. The distance between the electrodes was used as the scale for determining the plasma volume. At an interelectrode distance of 2 mm, the discharge gap was strongly overstressed. The nanosecond discharge at a pressure of  $p = 5\text{--}202$  kPa was fairly uniform [15].

The voltage pulses at the discharge gap and the discharge current were measured using a wide-band capacitive divider, a Rogovsky coil, and a 6-LOR 04 wide-band oscilloscope. The temporal resolution of this recording system was 2-3 ns. The pulse repetition rate varied in the range  $f = 35\text{--}1000$  Hz. The plasma radiation spectra were recorded using an MDR-2 monochromator, an FEU-106 photomultiplier, a direct current amplifier, and an electronic potentiometer. The radiation of the discharge plasma was analyzed in the spectral region of 200-650 nm. The plasma radiation registration system was calibrated by the radiation of a deuterium lamp in the spectral range of 200-400 nm and a gang lamp in the range of 400-650 nm. Oscillograms of radiation at the transitions of individual atoms and ions were recorded using an ELU 14 FS electronic linear multiplier, the temporal resolution of which was 1 ns. The pulsed electric power of an overstressed nanosecond discharge was determined by graphically multiplying the waveforms of voltage and current pulses. The time integration of the pulsed power made it possible to obtain energy in one electric pulse, which was introduced into the plasma.

Thin nanostructured films based on the degradation products of aluminum electrodes and air molecules were deposited during 2-3 hours of operation of the reactor on glass substrates that were installed at a distance of 3 cm from the center of the discharge gap. The resulting films were studied for light transmission in the visible wavelength range. The experimental technique and technique for recording the transmission spectra of synthesized films are described in [16].

## Results and Discussion

### Spatial, electrical and optical characteristics

The plasma volume depended on the repetition rate of voltage and current pulses and in the frequency range 10–150 Hz, it increased from 3 to 25 mm<sup>3</sup>. The discharge had a diffuse shape in the form of a ball. The most probable reason for obtaining a spatially homogeneous discharge in atmospheric pressure gases may be the preionization of the discharge gap by a runaway electron beam of about 130-150 ps duration and the accompanying X-ray radiation. It was shown in Beloplotov et al. [17] that even when using high-voltage pulses with a leading edge duration of about 200 ns, a runaway electron beam with an intensity of only one order of magnitude lower than even in the same discharge at an air pressure of 130 kPa is formed in a discharge plasma in atmospheric pressure air. The most characteristic waveforms of voltage and current pulses for an overstressed nanosecond discharge between aluminum electrodes in air are shown in (Figure 1).

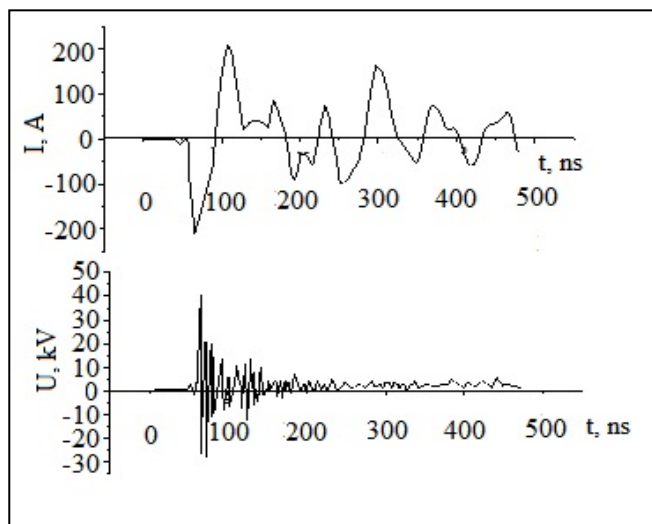


Figure 1. Oscillograms of voltage and current pulses at an air pressure of 101 kPa.

Due to the mismatch of the output resistance of the pulsed high-voltage modulator and the plasma resistance, the voltage pulse had the form of individual spikes with a duration of 5-10 ns. This mode of ignition of a subnanosecond high-voltage discharge between a metal electrode in the form of a needle and a flat metal plate (or

grid), when the total duration of a train of 10 nanosecond voltage pulses was 1–1.5  $\mu$ s, was used [10] to obtain plasma jets from a material electrodes. It is promising for applying thin metal films to solid substrates of finely dispersed powders based on electrode materials and degradation products of molecules of a gaseous medium. The maximum value of the positive and negative component of the current pulses reached 200 A, voltage amplitudes 30-40 kV. When air was replaced with argon, the form of the oscillograms did not change, the maximum values of the amplitude of the current and voltage of positive and negative polarity decreased, respectively, to 150 A and 15-20 kV.

Figure (2) presents the pulsed power and energy input into the plasma of an overstressed nanosecond discharge in air per pulse. With an increase in air pressure from 50 to 101 kPa, the maximum value of the pulsed electric discharge power increased from 3 to 6.5 MW, and the maximum energy input increased from 110 to 152.8 mJ. As the argon pressure increased from 50 to 101 kPa, the energy deposition into the plasma increased from 225.7 to 441.1 mJ.

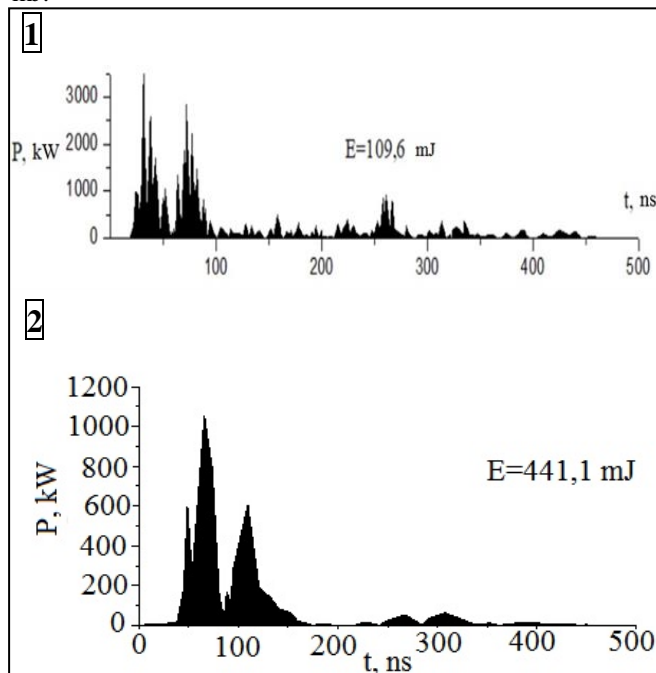


Figure 2. Pulsed power and energy input into a discharge per pulse at an air pressure of 50 kPa (1) and at an argon pressure of 101 kPa (2).

The emission spectra of a plasma of an overstressed nanosecond discharge between aluminum electrodes in air and argon are shown in (Figures 3 and 4). The experiments with argon, which were carried out in the same pressure range as with air, were performed to demonstrate the absence of emission bands of nanostructures of aluminum oxides in an inert gas plasma (where there are no oxygen carrier molecules). The spectra shown in (Figures 3. and 4), are registered under the same conditions for the excitation of the discharge and under the same conditions of registration.

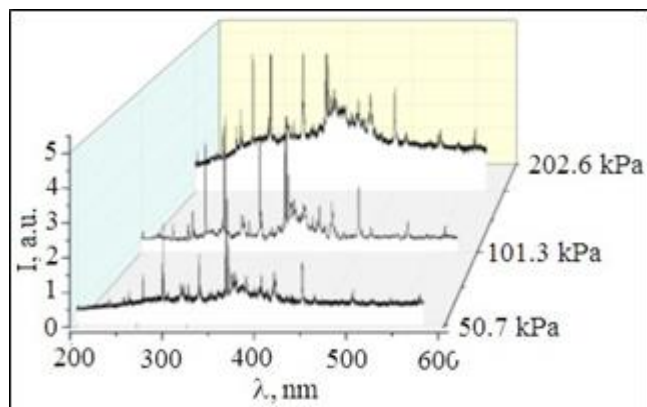


Figure 3. Plasma emission spectra of an overstressed nanosecond discharge at different air pressures (50.5, 101 and 202 kPa).

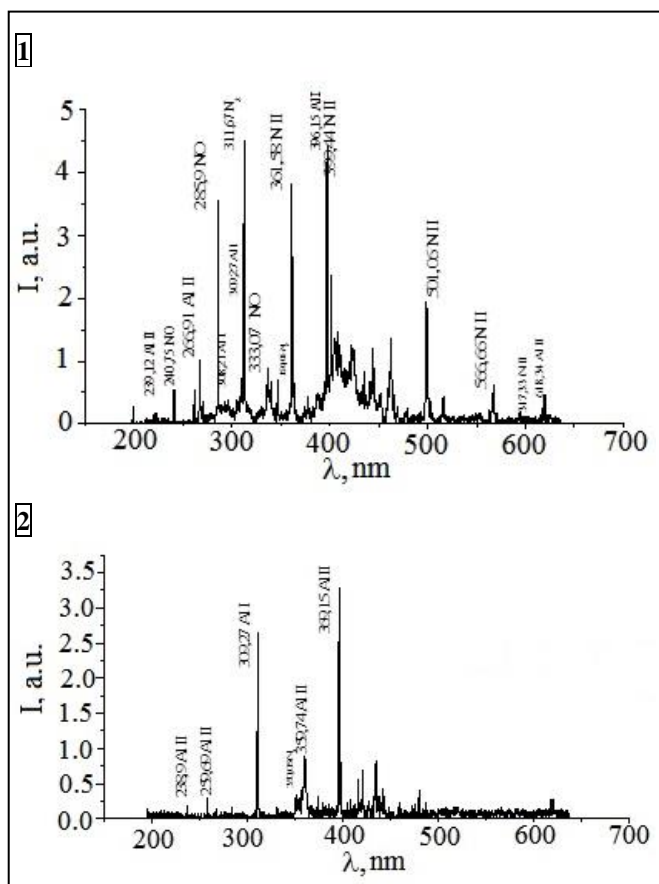


Figure 4. Plasma emission spectra of an overstressed nanosecond discharge with the interpretation of the most intense spectral lines and bands at an air pressure (1) and argon (2) of 101 kPa.

Therefore, the intensities of individual spectral lines and bands can be compared with each other. It can be seen from (Figure 3 and 4) that the intensity of the glow of the discharge plasma in air at all pressures studied by us exceeds the radiation intensity of spectral lines and discharge bands in argon. In the emission spectra of air plasma with a small admixture of aluminum vapor, radiation was detected at the transitions of the atom and singly charged ions of aluminum ion, nitrogen oxide radicals and nitrogen molecules, as in the emission spectra of a sub-

nanosecond plasma [10]. In an argon-based discharge, radiation was predominantly recorded at transitions of an atom and an aluminum ion. The most intense spectral lines of an atom and a singly charged aluminum ion, which were manifested in the plasma emission spectra, were as follows: (256.8 + 257.5 + 257.5); 265.3; 394.4; 396.2 nm Al I; 236.5; (247.5 + 247.6); 286.9; 622.6; (623.1 + 624.3) nm Al II. In the emission spectra of a plasma of an overstressed nanosecond discharge in air mixtures with an admixture of aluminum vapor (Figure 4), broad emission bands with peaks in the spectral ranges of 410–420 nm and 300–390 nm were recorded. The highest radiation intensity of these bands was obtained at an air pressure of 202 kPa. In argon-based mixtures, these bands are absent in the discharge emission spectra. Since a significant part of nitrogen is present in the air, in principle, in the discharge under study, the formation of inert gas nitride nanostructures is possible.

A comparison of the broadband emission spectra of an overstressed nanosecond discharge with the characteristic emission spectra of aluminum nitride nanostructures Silvera et al. [18] showed that they do not correlate with each other. Egorov et al. [19], characteristic electroluminescence spectra of anodic alumina are presented. Spectra in contact with solutions of different electrolytes were recorded at an oxidation current density of 5–15 mA / cm<sup>2</sup>. These spectra had the form of wide luminescence bands in the spectral range with maxima for different electrolytes in the spectral range of 480–550 nm. Based on this, the most probable source of broadband plasma radiation of the discharge under study can be aluminum oxide nanostructures.

Kortov et al. [6] was noted that in the photoluminescence spectrum of anion-defective single crystals and nanostructured ceramics based on aluminum oxide upon excitation of the corresponding samples by radiation with a wavelength of 205 nm, a wide emission band was observed with a maximum at a wavelength of 415 nm. This band coincides with that obtained in the present experiment. It is interpreted as the luminescence band of F centers (the 1S – 3P transition with a maximum of the emission spectrum at an energy of 3.0 eV and a decay time constant of 36–40 ms) [6, 20]. The results of studying the cathodoluminescence spectra of nanostructured alumina ceramics are also presented [6]. Cathodoluminescence was excited by a pulsed electron beam with a density of 1 A cm<sup>-2</sup>, an energy of 180 keV and a duration of 3 ns. The spectrum of this cathodoluminescence was similar to the spectrum recorded in our experiment at air pressures of 101–202 kPa. The main one was the emission band with a maximum at wavelengths of 410–420 nm (quantum energy 3.0 eV), which was adjoined by a wider short-wave band with maximum quantum energies at 3.4, 3.8, and 4.3 eV [6].

The ultraviolet photo and cathodoluminescence bands of nanostructured alumina ceramics are associated with the emission of  $F^+$  centers created by oxygen vacancies and have a relatively short decay time (0.6–1.0  $\mu\text{s}$ ) [6, 20]. **Figures (5 and 6)** present characteristic oscillograms of plasma radiation at transitions of radicals of nitric oxide and a singly charged nitrogen ion. At an air pressure of 50 kPa, the emission of the nitric oxide radical band appears with a delay of about 50 ns compared with the beginning of the current pulse, since it takes a certain time for the formation of excited NO radicals in the plasma.

The radiation pulse at the transition of the NO radical consisted of two maxima and had a total duration of 120–130 ns. At large times, it is likely that the discharge turned into a contracted state and no emission of NO radicals was observed. With an increase in air pressure to 101 kPa (**Figure 6**), the pulse amplitude and the duration of the radiation pulse at the transition of the nitric oxide radical increased (**Figure 6**). But at the same time, the duration of the first radiation maximum at the transition of the nitric oxide radical decreased and it became more pronounced. The longest radiation duration was recorded at the transition of a singly charged nitrogen ion (approximately 350 ns), which is characteristic of a recombining plasma of nanosecond discharges in air at atmospheric pressure [21].

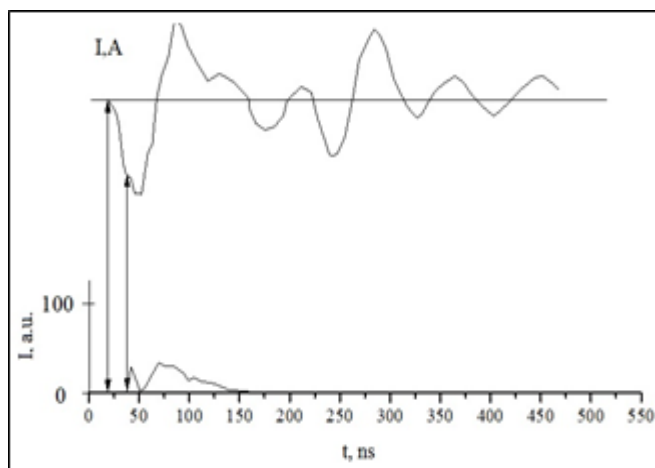


Figure 5. Oscillograms of current and radiation of the spectral line of a nitrogen ion 361 nm (N II) for a discharge in air at a pressure of 50 kPa.

Transmission spectra in the visible wavelength range of nanostructured films based on copper and aluminum synthesized on a glass substrate are presented in (**Figure 7**). As can be seen from (**Figure 7**) the obtained film is characterized by weak transmission of radiation in the visible wavelength region. According to Gasenkova *et al.* [20], films based on nanostructured alumina ceramics are practically not transparent to the visible region of the spectrum; their transmittance begins to increase in the spectral range of 0.8–2.0  $\mu\text{m}$  from 1-3 to 25%.

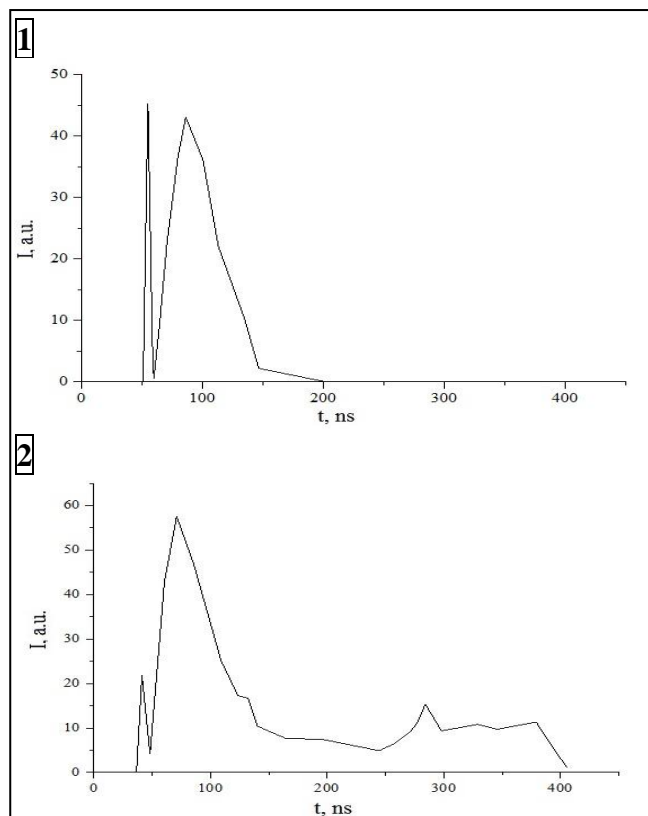


Figure 6. Oscillograms of the emission of the band 333.5 nm (NO) (1) and the spectral line of a singly charged nitrogen ion 361 nm (N II) (2) in an overstressed nanosecond discharge in air (p - 101 kPa).

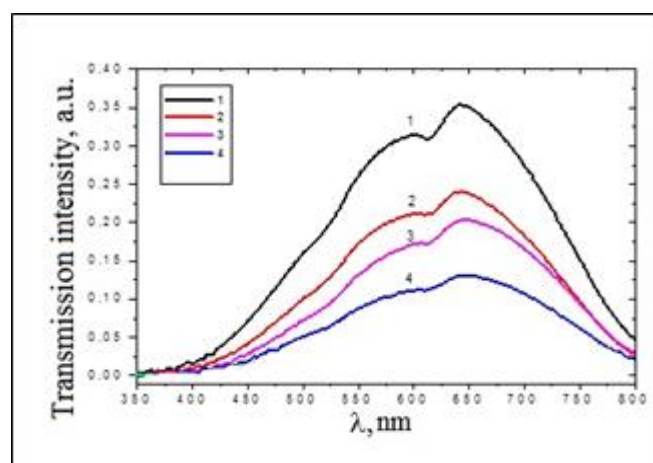


Figure 7. The transmission spectra of films based on copper and aluminum in the spectral region of 350-800 nm (band lamp): 1 - a pure glass substrate, 2 - a nanostructured copper film synthesized in argon at a pressure of 101 kPa, 3 - a nanostructured copper oxide film synthesized in air at a pressure of 101 kPa, 4 - a film obtained by sputtering aluminum electrodes in air at a pressure of 101 kPa; the repetition rate of voltage and current pulses is 40 Hz, and the sputtering time is 3 hours.

### Plasma parameters

The discharge plasma parameters for mixtures of aluminum and air vapor and aluminum and argon vapor at atmospheric pressure (component ratio 30 Pa: 101 kPa, respectively) were determined numerically and calculated as

the total integrals of the electron energy distribution function (EEDF) in the discharge. EEDFs were found numerically by solving the Boltzmann kinetic equation in the two-term approximation. EEDF calculations were carried out using the program [22]. Based on the EEDFs obtained, the mean electron energies, electron temperatures, electron drift velocities, electron densities, excitation rate constants of the energy levels of aluminum atoms, and specific discharge losses on elastic and inelastic collisions of electrons with atoms and molecules of both mixtures are determined depending on the magnitude of the reduced electric field (the ratio of the electric field (E) to the total concentration of atoms of aluminum, argon and molecules of nitrogen, oxygen and carbon dioxide for (N)). The variation range of the parameter  $E/N = 1\text{-}1000\text{ Td}$  ( $1 \cdot 10^{-17} - 1 \cdot 10^{-14}\text{ V} \cdot \text{cm}^2$ ) included the values of the reduced electric field that were realized in the experiment. For gas-vapor mixtures Al - Air and Al - Ar, these reduced electric fields were 820 Td and 205 Td in the time ranges of 50-100 ns and 100 -480 ns of voltage pulses, respectively (**Figure 1**). The following processes are taken into account in the integral of collisions of electrons with atoms and molecules: elastic scattering of electrons by aluminum atoms, excitation of energy levels of aluminum atoms (threshold energies of 3.1707 eV, 2.9032 eV, 4.1463 eV, 4.2339 eV, 4.1296 eV, 5.1220 eV), ionization of aluminum atoms ( threshold energy 6.0000 eV); elastic electron scattering by argon atoms, excitation of the energy level of argon atoms (threshold energy 11.50 eV), ionization of argon atoms (threshold energy, 15.80 eV); elastic scattering and excitation of energy levels of nitrogen molecules: rotational - threshold energy of 0.020 eV, vibrational (threshold energy: 0.290 eV, 0.291 eV, 0.590 eV, 0.880 1.170, 1.470, 1.760, 2.060, 2.350; electronic: 6.170 eV, 7.000, 7.350, 7.360, 7.800, 8.160, 8.400, 8.550, 8.890, 11.03, 11.87, 12.25, 13.00, ionization (threshold energy - 15.60 eV); elastic scattering and excitation of energy levels of oxygen molecules: vibrational (threshold energies: 0.190 eV, 0.380 eV , 0.570 eV, 0.750 eV), electronic (threshold energy: 0. 977 eV, 1.627 eV, 4.500 eV, 6.000 eV, 8.400 eV, 9.970 eV, dissociative electron attachment (threshold energy - 4.40 eV), ionization (threshold energy - 12.06 eV); elastic scattering and excitation of energy levels of carbon dioxide molecules: vibrational (threshold energies: 0.083 eV, 0.167 eV, 0.252 eV, 0.291 eV, 0.339 eV, 0.422 eV, 0.505 eV, 2.5 eV ), electronic (threshold energy: 7.0 eV, 10.5 eV), dissociative electron attachment (threshold energy 3.85 eV), ionization (threshold energy 13.30 eV). Data on the absolute values of the effective cross sections of these processes, as well as their dependences on electron energies, were taken from the databases and L.L. Shimon [22-25]. **Figure (8)** shows the dependences of the mean electron energy in the plasma of the vapor-gas mixture Al: Air = 30: 101000 and Al: Ar = 30: 101000 at a total pressure of  $p = 101.030\text{ kPa}$ .

101000 at a total pressure  $p = 101.030\text{ kPa}$  on the reduced electric field strength.

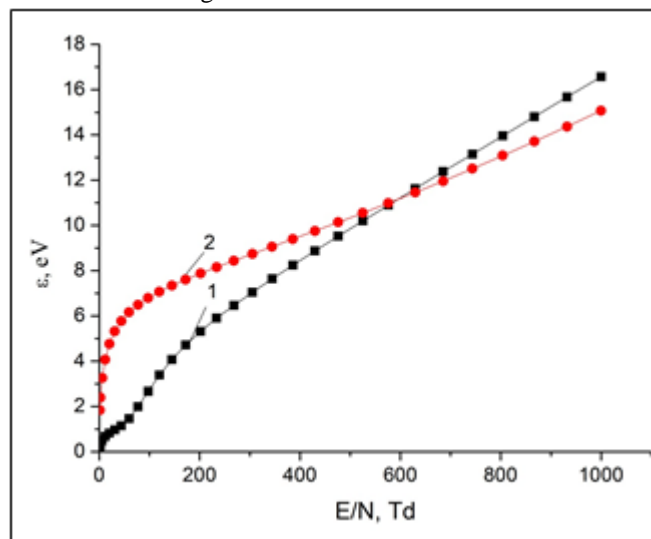


Figure 8. Dependences of the mean electron energy in the plasma of a vapor-gas mixture on the reduced electric field strength: 1-Al - air = 30: 101000, 2-Al -Ar = 30: 101000 at a total pressure of  $p = 101.030\text{ kPa}$ .

The mean energy of the discharge electrons for the vapor-gas mixture aluminum-air = 30Pa - 101 kPa almost linearly increases from 0.1364 eV to 16.57 eV (**Figure 8** (1)), and for the aluminum-argon mixture it also increased from 1.838 eV to 15.07 eV (**Figure 8** (2)) with an increase in the reduced electric field strength from 1 Td to 1000 Td. At the same time, a regularity was observed in the increased rate of its change in the ranges of 30–80 Td and 1–30 Td for mixtures of the first and second, respectively. For the reduced electric field strength range 205 Td - 820Td at which experimental studies of the electric and optical characteristics of the discharge were carried out, the average electron energies varied between 5.323-13.96 eV for the vapor-gas mixture aluminum-air and 7.882 -13.09 for the mixture aluminum-argon. Their highest energies corresponded to the values of 62.52 eV - 249.0 eV for the first mixture, and for the second mixture 71.14 eV - 282.8 eV.

**Table (1)** presents the results of modeling the transport characteristics of electrons: mean energies in  $\epsilon$ , temperature  $T\text{ K}$ , and drift velocity  $V_{dr}$  and electron concentration for two mixtures of aluminum vapor with air and aluminum vapor with argon. The temperature and electron drift velocity (**Table 1**) decreases from 161936 K to 61 746.8 K and from  $6 \cdot 10^5\text{ m/s}$  to  $2 \cdot 10^5\text{ m/s}$  for the first mixture, and for the second mixture from 151844 to 91431.2 and  $4 \cdot 10^4$  to  $1.4 \cdot 10^4$  when changing the reduced electric field strength from 820 Td to 205 Td, respectively. The values of electron concentration increase from  $1.1 \cdot 10^{20}\text{ m}^{-3}$  to  $1.6 \cdot 10^{20}\text{ m}^{-3}$  at a current density  $1.02 \cdot 10^7\text{ A/m}^2$  and  $5.1 \cdot 10^6\text{ A/m}^2$  on the surface of the electrode of the radiation source ( $0.196 \cdot 10^{-4}\text{ m}^2$ ) for both mixtures.

Table 1. Transport characteristics of electrons for the mixture: Al-Air=30 Pa – 101 kPa and Al - Ar=30 Pa – 101 kPa

Mixture: - Al-Air=30 Pa – 101 kPa				
E/N, Td	$\epsilon$ , eV	$T^0$ K	$V_{dr.}$ , m/s	$N_e$ , $m^{-3}$
1	0.1364	18362	$6.2 \cdot 10^3$	$5.1 \cdot 10^{21}$
97	2.672	30995,2	$2.5 \cdot 10^3$	$1.3 \cdot 10^{22}$
205	5.323	61746,8	$2 \cdot 10^5$	$1.6 \cdot 10^{20}$
820	13.96	161936	$6 \cdot 10^5$	$1.1 \cdot 10^{20}$
1000	16.57	192212	$5.4 \cdot 10^4$	$1.1 \cdot 10^{21}$
Mixture: Al - Ar=30 Pa – 101 kPa				
E/N, Td	$\epsilon$ , eV	$T^0$ K	$V_{dr.}$ , m/s	$N_e$ , $m^{-3}$
1	1.838	4431	$1.4 \cdot 10^5$	$2.3 \cdot 10^{20}$
97	6.795	78822	$1.7 \cdot 10^4$	$1.9 \cdot 10^{21}$
205	7.882	91431,2	$1.4 \cdot 10^4$	$1,6 \cdot 10^{20}$
820	13.09	151844	$4 \cdot 10^4$	$1.1 \cdot 10^{20}$
1000	15.07	174812	$4.8 \cdot 10^4$	$1.3 \cdot 10^{21}$

Figure (9) presents the dependence of the specific power of the discharge losses on both elastic (1, 2) and inelastic (3,4) collisions of electrons with mixture components in a gas-discharge plasma on the reduced electric field strength. An increase in power is observed with increasing values of the reduced electric field, both for elastic processes and for inelastic ones. In addition, higher values of specific power of discharge losses are observed for inelastic collisions of electrons with atoms and molecules in a mixture of aluminum and air vapors (Figure 9, Table 2).

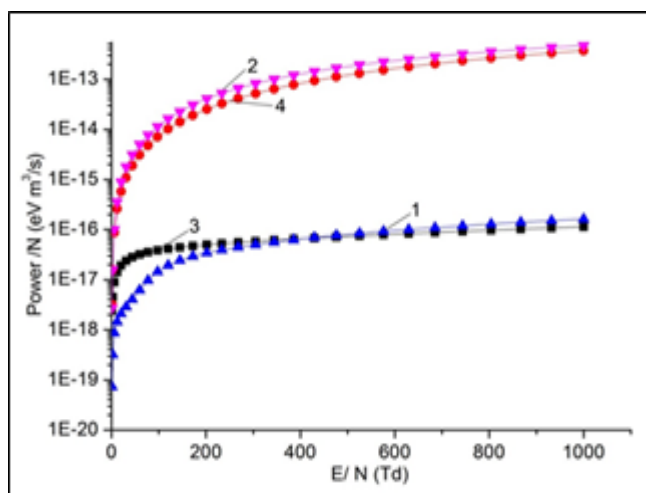


Figure 9. The specific discharge power for elastic (1) and inelastic (2) processes per unit of the total concentration of the mixture vs the reduced electric field strength for the aluminum-air mixture and for elastic (3) and inelastic (4) processes for the aluminum-argon mixture.

Figure (10) and Table (3) present the results of numerical simulation of the dependence of the excitation rate constants of the spectral lines of aluminum atoms on the reduced

electric field strength in mixtures of aluminum and air and aluminum and argon vapor for the ratio of partial pressures in mixtures of 30 - 101000 Pa at a total pressure of the mixture  $P = 101030$  Pa. The rate constants are characterized by a high value, which is associated with the values of the absolute effective cross sections of the corresponding processes. In the range of reduced electric field strength 205 Td - 820 Td, at which experimental studies of the electrical and optical characteristics of the discharge were carried out, they were in the range of  $k \approx 10^{-16} - 10^{-15} m^3/s$ .

Table 2. Elastic and inelastic power loss /N (eV  $m^3/s$ ) for mixtures Al-Air=30 Pa – 101 kPa and Al - Ar=30 Pa – 101 kPa

Mixture Al-Air=30 Pa – 101 kPa		
E/N, Td	Elastic, Power /N (eV $m^3/s$ )	Inelastic, Power /N (eV $m^3/s$ )
205	3,448E-17	4,091E-14
820	1,290E-16	3,559E-13
Mixture Al - Ar=30 Pa – 101 kPa		
E/N, Td	Elastic, Power /N (eV $m^3/s$ )	Inelastic, Power /N (eV $m^3/s$ )
205	4,995E-17	2,535E-14
820	9,709E-17	2,658E-13

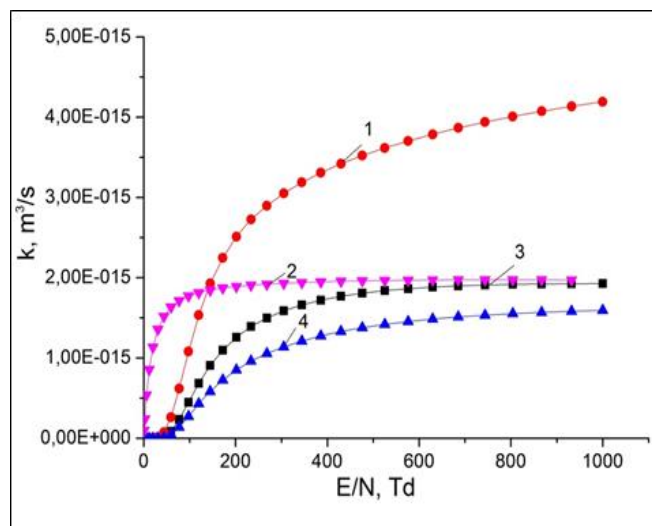


Figure 10. Dependences of the rate constants of excitation of the spectral lines of aluminum atoms on the reduced electric field strength in a plasma on a mixture of aluminum and air vapors: 30: 101000 Pa at a total pressure of the mixture  $P = 101030$  Pa and aluminum and argon 30: 101000 Pa at the total pressure of the mixture  $P = 101030$  Pa : 1-  $\lambda = 396.15$  nm ( $E_{thr.} = 3.17$  eV) for an aluminum-air mixture, 2- $\lambda = 309.27$ nm ( $E_{thr.} = 4.23$  eV) for an aluminum-argon mixture, 3- $\lambda = 309.27$ nm ( $E_{thr.} = 4.23$  eV ) for an aluminum-air mixture, 4- $\lambda = 308.21$ nm ( $E_{thr.} = 4.13$  eV) for an aluminum-air mixture.

Table 3. The rate constants of the excitation of the spectral lines of aluminum atoms for the values of the reduced electric field strength in a plasma on a mixture of aluminum and air vapor: 30 - 101000 Pa and aluminum and argon: 30 - 101000 Pa at a total pressure of the mixture  $P = 101030$  Pa.

E/N, Td	Mixture Al-Air			Mixture Al-Ar
	$\lambda = 396.15$ nm	$\lambda = 309.27$ nm	$\lambda =$ 308.21 nm	$\lambda = 309.27$ nm
205	2.51E-15	1.26E-15	8.52E-16	1.89E-15
820	4.01E-15	1.92E-15	1.55E-15	1.98E-15

### Limitations methods

To reduce the body effects and to obtain better films, in the future it is necessary to switch to the subnanosecond mode of operation of the reactor with a total voltage pulse duration of the order of 1 ns. This will contribute to the full implementation of the ectonic mechanism of aluminum atomization and improve the control of the film deposition process.

### Conclusions

Thus, it was found that a plasma of an overstressed nanosecond discharge between aluminum electrodes at air pressures of 50–202 kPa, a pulsed discharge power of 3–6.5 MW, and an energy input of one pulse of 110–153 mJ is a source of electroluminescence of aluminum oxide nanoparticles in the form of a wide band, which is in the spectral range of 300–430 nm; upon deposition of degradation products of electrodes and air molecules in a plasma on a glass substrate, films based on aluminum oxides were obtained, which are characterized by low transparency in the visible region of the spectrum.

Numerical simulation of plasma parameters in a mixture of aluminum and air vapor established that for the reduced electric field strength of 820 Td - 205 Td, at which experimental studies of the electric and optical characteristics of the discharge were carried out, the mean electron energies varied between 13.96 and 5.323 eV, their highest energies corresponded to the values of 249.0 eV - 62.52 eV. In a mixture of aluminum and argon vapor, these values of the discharge parameters varied within 13.09 eV - 7.882 eV and 282.8 eV - 71.14 eV, respectively. The electron concentration was  $1.1 \cdot 10^{20} \text{ m}^{-3}$  -  $1.6 \cdot 10^{21} \text{ m}^{-3}$  at current density  $1.02 \cdot 10^7 \text{ A/m}^2$  and  $5.1 \cdot 10^6 \text{ A/m}^2$  at the surface of the aluminum electrode ( $0.196 \cdot 10^{-4} \text{ m}^2$ ).

The excitation rate constants of the spectral lines of aluminum atoms  $\lambda=396.15$  nm,  $\lambda=309.27$  nm,  $\lambda=308.21$  nm are in the range of  $(4.009- 2.511) \cdot 10^{-15} \text{ m}^3/\text{s}$ ,  $(1.918 - 1.259) \cdot 10^{-15} \text{ m}^3/\text{s}$ ,  $(1.553- 0.852) \cdot 10^{-15} \text{ m}^3/\text{s}$ ,  $(1.975- 1.975) \cdot 10^{-15} \text{ m}^3/\text{s}$ , respectively. The maximum value of the excitation rate constant of the spectral line of aluminum atoms  $\lambda=396.15$  nm was  $(4.009 \cdot 10^{-15}) \text{ m}^3 \text{ s}$  for the reduced

electric field strength of 820 Td in a mixture of aluminum and air.

The specific discharge power loss for inelastic and elastic collisions of electrons with atoms and molecules, which were part of the working mixtures of a gas-discharge plasma, per unit total concentration of the mixture increased with increasing reduced electric field for both inelastic and elastic processes. Its maximum value was for inelastic processes in a mixture of aluminum and air vapor was equal to  $3.559 \cdot 10^{-13} \text{ eV m}^3/\text{s}$  for a reduced electric field strength of 820 Td.

### References

1. Bityurin VA, Efimov AV, Grigorenko AV, Goryachev SV, Klimov AI, Chinnov VF. Plasma stimulation of aluminum burning in water vapor. Modern Science. Collection of Research Papers.2011 2(7): 47.
2. Bityurin VA, Grigorenko AV, Efimov AV, Klimov AI, Korshunov OV, Kutuzov DS, Chinnov VF. Spectral and kinetic analysis of heterogeneous gas discharge plasma in the flow of an Al, H<sub>2</sub>O, and Ar mixture. High Temperature. 2014 Jan 1;52(1):1-1.
3. Shkolnikov EI, Beetle AZ, Bulychev BM, Larichev MN, Ilyukhina AV, Vlaskin MS; edited by A.E. Scheindlin. Oxidation of aluminum with water for efficient power generation. Joint Institute for High Temperatures RAS. M.: Science. 173 p.
4. Mesyats GA. Ecton-electron avalanche from metal. Uspekhi fizicheskikh nauk. 1995 Jun 1;165(6):601-26.
5. Walters JP, Malmstadt HV. Emission Characteristics and Sensitivity in a High-Voltage Spark Discharge. Analytical Chemistry. 1965 Nov 1;37(12):1484-503.
6. Kortov VS, Ermakov AE, Zatselin AF, Uimin MA, Nikiforov SV, Mysik AA, Gaviko VS. Specific features of luminescence properties of nanostructured aluminum oxide. Physics of the Solid State. 2008 May 1;50(5):957.
7. Zorenko Y, Fabisiak K, Zorenko T, Mandowski A, Xia Q, Batentschuk M, Friedrich J, Zhusupkalieva G. Comparative study of the luminescence of Al<sub>2</sub>O<sub>3</sub>: C and Al<sub>2</sub>O<sub>3</sub> crystals under synchrotron radiation excitation. Journal of luminescence. 2013 Dec 1;144:41-4.
8. Abyzov AM. Aluminum oxide and alumina ceramics (Review). Part 1. Properties of Al<sub>2</sub>O<sub>3</sub> and industrial production of dispersed Al<sub>2</sub>O<sub>3</sub>. NOVYE OGNEUPORY (NEW REFRACTORIES). 2019 Apr 26(1):16-23.
9. Ananchenko DV, Nikiforov SV, Ramazanova GR, Batalov RI, Bayazitov RM, Novikov HA. Luminescence of F-Type Defects and Their Thermal Stability in Sapphire Irradiated by Pulsed Ion Beams. Optics and Spectroscopy. 2020 Feb;128:207-13.
10. Beloplotov DV, Tarasenko VF, Lomaev MI. Luminescence of aluminum atoms and ions in a repetitively pulsed discharge initiated by runaway electrons in nitrogen. Optics of the atmosphere and ocean 2016 29 (2): 96.
11. Shuaibov AK, Minya AY, Malinina AA, Malinin AN, Danilo VV, Sichka MY, Shevera IV. Synthesis of copper oxides nanostructures by an overstressed nanosecond discharge in atmospheric pressure air

- between copper electrodes. *Am. J. Mech. Mater. Eng.* 2018 May 7;2(8).
12. Shuaibov AK, Minya AI, Gomoki ZT, Danylo VV, Pinzenik PV. Characteristics of High-Current Pulse Discharge in Air with Ectonic Mechanism of Copper Vapor Injection into a Discharge Gap. *Surface Engineering and Applied Electrochemistry.* 2019 Jan 1;55(1):65-9.
  13. Shuaibov OK, Malinina AO, Malinin OM. New gas discharge methods for the production of selective ultraviolet and visible radiation and synthesis of nanostructures of transition metal oxides. Monograph. Uzhhorod. Publishing House of UzhNU "Hoverla. 2019.
  14. Shuaibov AK, Minya AY, Hrytsak RV, Malinina AA, Malinin AN. Characteristics of an Overstressed Discharge of Nanosecond Duration between Electrodes of Chalcopyrite in High Pressure Nitrogen. *Advances in Nanoscience and Nanotechnology* 2020 4(1): 1.
  15. Tarasenko VF. Runaway electrons preionized diffuse discharge, New York: Nova Science Publishers Inc., 2014. -578 p.
  16. Holovey VM, Popovych KP, Prymak MV, Birov MM, Krasilinets VM, Sidey VI. X-ray induced optical absorption in Li<sub>2</sub>B<sub>4</sub>O<sub>7</sub> and Li<sub>2</sub>B<sub>4</sub>O<sub>7</sub>: Cu single crystals and glasses. *Physica B: Condensed Matter.* 2014 Oct 1;450:34-8.
  17. Beloplotov DV, Tarasenko VF. On the influence of a cathode shape on the parameters of current pulses of runaway electron beams in a gas discharge when applying voltage pulses with a rise time of 200 ns. *In Journal of Physics: Conference Series* 2019 Nov (Vol. 1393, No. 1, p. 012004). IOP Publishing.
  18. Silveira E, Freitas Jr JA, Glembocki OJ, Slack GA, Schowalter LJ. Excitonic structure of bulk AlN from optical reflectivity and cathodoluminescence measurements. *Physical Review B.* 2005 Jan 7;71(4):041201.
  19. Egorov AE, Chernyshev VV. Electroluminescence spectra of anodic alumina in various electrolytes. *Bulletin of Voronezh State University. Series. Physics mathematics* 2005 2:8.
  20. Gasenkova IV, Mukhurov NI, Vakhioh Yasin Mohsin. Optical properties of anodized aluminum substrates as a basis for threshold detectors. *Reports of BSUIR* 2016 2 (96): 114.
  21. Van der Horst RM, Verreycken T, Van Veldhuizen EM, Bruggeman PJ. Time-resolved optical emission spectroscopy of nanosecond pulsed discharges in atmospheric-pressure N<sub>2</sub> and N<sub>2</sub>/H<sub>2</sub>O mixtures. *Journal of Physics D: Applied Physics.* 2012 Aug 10;45(34):345201.
  22. <http://www.bolsig.laplace.univ-tlse.fr> .
  23. Shimon LL. Influence of autoionization states on the population of energy levels of atoms of the aluminum subgroup. *Scientific Bulletin of UzhNU. Physics Series* 2007 20:55-61.
  24. <http://www.ioffe.ru/ES/Elastic/data2.html>
  25. [https://physics.nist.gov/cgi-bin/Ionization/ion\\_data.php?id=Al&ision=I&initial=&total=Y](https://physics.nist.gov/cgi-bin/Ionization/ion_data.php?id=Al&ision=I&initial=&total=Y)